MULTIDISCIPLINARY SCIENCE JOURNAL

RESEARCH ARTICLE
Published Online: March 1, 2025
https://doi.org/10.31893/multiscience.2025370

Understanding *Sonic hedgehog* (*Shh*) expression and its distribution in common house gecko (*Hemidactylus platyurus*) tail regeneration

Maytia Pratiwisitha[ab] | Ria Margiana[c] ✉ | Mohamad Sadikin[d] | Ahmad Aulia Jusuf[e]

[a]Master's Programme in Biomedical Sciences, Faculty of Medicine, Universitas Indonesia, Indonesia.
[b]Department of Biomedical Sciences, Faculty of Medicine and Health Sciences, Universitas Sultan Ageng Tirtayasa Banten, Indonesia.
[c]Department of Anatomy, Faculty of Medicine, Universitas Indonesia, Indonesia.
[d]Department of Biochemistry and Molecular Biology, Faculty of Medicine, Universitas Indonesia, Indonesia.
[e]Department of Histology, Faculty of Medicine, Universitas Indonesia, Indonesia.

Abstract Mammals, especially humans, have limited regenerative abilities compared to lower organisms. The common house gecko (*Hemidactylus platyurus*) exhibits high regenerative capacity and closer evolutionary relationship to mammals than other highly regenerative species. Observing the regeneration process in house gecko reveals insights into the biological mechanisms underlying tissue regeneration after injury. *Sonic hedgehog* (*Shh*) pathway is essential for intercellular communication during development and regeneration. In this study, *Shh* expression and its distribution during the tail regeneration in the common house gecko (*Hemidactylus platyurus*) were examined to understand the molecular mechanisms regulating regeneration. A total of 28 house geckos were divided into 7 groups based on sampling time. Autotomy procedures were conducted for all groups. The tails were allowed to regenerate, measured using graph paper, and cut to be analyzed. *Hematoxylin-eosin* and immunohistochemical staining using anti-*Shh* primary antibody were conducted to observe the microscopic structure and *Shh* expression. Statistical analyses were conducted to analyze the obtained data. Tail elongation was observed throughout the regeneration process. *Shh* expression is evident in both original and regenerated tails, commencing on day 1 post autotomy, peaking on day 14, stabilizing until day 21, and gradually decreasing by day 30. Statistical analysis showed significant differences on tail length measurement and Shh expression between groups ($p < 0.001$). The results showed strong positive correlation between *Shh* expression and regenerated tail length from day 1 to day 14 (R=0.818; p<0.001). Additionally, strong negative correlation was observed between *Shh* expression and regenerated tail length from day 21 to day 30 (R=-0.852; p<0.001). *Shh* protein is detected in a variety of cell types within both original and regenerated tail tissues. It plays critical role in maintaining tissue homeostasis in adult tissues and facilitating the proliferation, migration, and differentiation of blastema cells in response to injury.

Keywords: *Sonic hedgehog*, morphogen, tissue regeneration, common house gecko, animal model, regenerative medicine

1. Introduction

Tissue and organ injuries in humans remain a major challenge in healthcare. Various factors contribute to these injuries, such as congenital abnormalities, trauma, and disease. However, regenerative ability in mammals, especially in the human body, is still limited compared with that in lower organisms at the taxonomic scale (Dzobo et al., 2018). Some organisms, such as many plants and planarians, can regenerate almost entirely, whereas others, such as salamanders and fish, can replace complex structures (Ninov & Yun, 2015). Thus, regenerative medicine holds promise for enabling the repair and replacement of diverse tissues and organs. Regenerative medicine has significant potential to support and enhance the effectiveness of conventional medicine provided to humans (Moradi et al., 2015).

Regeneration is a complex process that reactivates developmental mechanisms in adults to restore lost or damaged tissues after injury through cell proliferation, migration, differentiation, and morphogenesis. Regenerative capacity varies significantly among species. This regenerative potential is correlated with the regenerative abilities of metazoan ancestors (Barresi & Gilbert, 2021). Research on the natural regeneration process in animals with high regenerative capacity is still extensive. Lizards can shed their tails when threatened. During autotomy, bleeding occurs along with damage to nerves, muscles, and bones. This natural phenomenon provides insight into the mechanisms of vascular control, wound healing, and tissue remodeling (Lozito & Tuan, 2017). The autotomy process activates multiple cellular responses, including blastema-mediated cell proliferation, angiogenesis, remodeling, and tissue regeneration (Nagumantri et al., 2021).

The common house gecko (*Hemidactylus platyurus*) is a reptile with high regenerative, ability that is commonly found in homes throughout Asia. Compared with other highly regenerative animals, this species is well-known for its ability to

 Received: November 4, 2024 | Accepted: December 9, 2024

undergo autotomy and has a closer evolutionary relationship with mammals. Previous research has shown that the tail tissue of the common house gecko consists of a complex tissue structure in both the original and regenerated tails (Novianti et al., 2019). The processes of autotomy and regeneration in the common house gecko (*Hemidactylus platyurus*) are intriguing topics for observing the biological mechanisms of tissue regeneration following injury.

In animals, epimorphic regeneration starts with an undifferentiated mass called a blastema, which grows and differentiates during morphogenesis to restore lost tissues. This process relies on several developmental pathways, indicating that a conserved mechanism is shared between embryonic development and tissue regeneration (Goldman & Poss, 2020). The Hedgehog (*Hh*) pathway is one of the signaling pathways extensively utilized during development for intercellular communication. Hedgehog is a key morphogen involved in organogenesis across all organs, including roles in regeneration and homeostasis. In mammals, the Sonic hedgehog (*Shh*) protein plays a significant role in cell type specification within the nervous system and limb patterning (Bangs & Anderson, 2017). In addition to regulating developmental processes in multicellular organisms, the Shh signaling pathway also plays a crucial role in postembryonic tissue regeneration and repair processes (Carballo et al., 2018).

Shh plays a critical role in the tail regeneration process in lizards by driving cartilage tissue formation and patterning. In lizard tail tissue, *Shh* is secreted primaly by ependymal tube neural stem cells. This secretion of *Shh* aids in the formation of a cartilage tube structure surrounding the spinal cord, facilitating the functional structure of the tail. The *Shh* signaling pathway establishes an environment essential for blastema cell proliferation and enables the differentiation process into various cell types that form lizard tail tissues (Lozito et al., 2021).

In this study, various cell types composing the tail tissue of the common house gecko (*Hemidactylus platyurus*), an animal model, that expresses *Shh* during the regeneration process, were observed. This regeneration study aims to understand the molecular mechanisms that control regeneration and its distribution, with a particular focus on the *Shh* morphogen, a conserved regenerative pathway, which could help to identify therapeutic targets to treat human injuries and degenerative diseases. Understanding tissue regeneration is crucial for advancements in regenerative medicine, including applications in wound healing, organ repair, and even limb regeneration.

2. Materials and methods

2.1. Research methods

The research method used a descriptive-analytical experimental design to analyze the expression and distribution of the *Shh* protein in house gecko tail tissue regeneration. The research procedures included animal acclimatization, autotomy, tail length measurement, regenerated tail tissue sampling, hematoxylin-eosin staining, and immunohistochemical staining for data collection and statistical analyses. The research was performed in the Animal Laboratory of Chemistry Department, the Department of Anatomy, the Department of Histology, and the laboratory of the Department of Biochemistry & Molecular Biology, Faculty of Medicine, Universitas Indonesia, from June to October 2024.

2.2. Subjects

The subjects of this study were common house geckos of the species *Hemidactylus platyurus*, characterized by a flat tail with serrated edges, which were identified by the National Research and Innovation Agency (BRIN) in Cibinong. The sample size in this study was calculated via *Federer's* formula: $(n-1)(t-1) \geq 15$, where *t* is the number of treatments, totaling 7 treatment groups, resulting in a total sample size of 28 house geckos. The treatment group was divided on the basis of the day of sampling, with group 0 as the original tail group, followed by the regenerated tail group on days 1 (group 1), 3 (group 3), 7 (group 7), 14 (group 14), 21 (group 21), and 30 (group 30). The characteristics of the house geckos used in this research included body weight (5±0.5 g), body length (10–13 cm), and tail length (5.0–6.0 cm).

2.3. Animal acclimatization

Animal acclimatization was conducted for 7 days before treatment. The animals were placed in seven separate cages according to treatment group. Each cage contained four house geckos. The cages were kept at room temperature (24-28°C) with a 12-hour light and dark cycle. The cages were made of thick transparent plastic (26x18x9 cm^3), with air holes on the walls and roof. There was an opening on the roof to facilitate animal handling, as well as the provision of food and water. The food provided was free-moving insects and water, which was supplied in a small bowl and substituted daily. The cages were lined with husks and dry leaves. Transverse wood was added to support the movement of the house geckos, mimicking their natural habitat. The cages were regularly cleaned, and the lining was changed every three days. The gecko groups were marked by separating the cages and placing numbers on their heads, which were routinely updated to anticipate skin shedding of the house geckos.

2.4. Autotomy procedure

The autotomy procedure was performed on all the samples. Autotomy was performed by holding the body of the house gecko. The tail was broken off manually at the autotomy plane, approximately 1 cm from the base of the original tail or the caudal part of the cloaca. Four original tails were measured and analyzed as the original tail group (0). The tails of the other house gecko groups were allowed to grow, their length was measured, and regenerated tail samples were collected at the specified time for each group.

2.5. Tail length measurement

Original tails were measured from the base to the tip of the original tails. Moreover, regenerated tail length measurements of the house geckos were taken according to the group divisions on days 1, 3, 7, 14, 21, and 30. Measurements were made from the base or autotomy point to the tip of the regenerated tail. The length was measured on graph paper using millimeter (mm) units. The body of the house gecko was placed horizontally on graph paper, and measurements of the regenerated tail length were taken once the gecko had calmed down.

2.6. Sampling procedure

The sampling procedures were adjusted according to the treatment groups on days 1, 3, 7, 14, 21, and 30. Before sample collection, local anesthesia was applied to the regenerated tail using an ethyl chloride spray on the sampling area. After waiting a few seconds for the sensory response of the house gecko's tail to diminish, the sample was collected by cutting the regenerated tail tissue in transverse and longitudinal sections via a sterile 11 blade, 0.5 cm from the base of the original tail or the cloaca. Each sample of regenerated tails was stored in 70% formalin and then used for histological and immunohistochemical analysis.

2.7. H&E staining

Regenerated tail samples from days 0, 1, 3, 7, 14, 21, and 30 were preserved in 70% formalin for 24 hours. The tissues were dehydrated in graded alcohols and cleared with xylene. The tail tissues were then embedded in liquid paraffin and allowed to solidify into paraffin blocks to be sectioned with a microtome at a thickness of 4–5 µm. The tissue sections were mounted on glass slides and incubated for 24 hours. The sections were then subjected to hematoxylin-eosin (H&E) staining.

2.8. Immunohistochemical staining

Regenerated tail tissue samples were sectioned via a microtome, placed on glass slides, deparaffinized, and prepared for immunohistochemical (IHC) staining. The primary antibody used was rabbit anti-*Shh* antibody at a 1:100 dilution (NBP2-22139 Sonic Hedgehog/*Shh* Antibody-BSA Free) to detect Shh expression in house gecko (*Hemidactylus platyurus*) tail tissue. N-Histone Simple Stain MAXPO® was used as a universal anti-rabbit immunoperoxidase polymer, which binds to the primary antibody. The DAB chromogen binds directly to the polymer and is visualized via *Indomicroview* software.

2.9. Immunohistochemical analysis of Shh expression

Immunohistochemical analysis was performed via *ImageJ* software. The data were semiquantitatively analyzed by calculating the density of areas with positive IHC staining, which are marked in brown. The brown color indicates the binding between the Shh protein and the anti-*Shh* primary antibody. The average density of positively stained areas per sample was calculated in five fields of view at 40x10 magnification.

2.10. Statistical analysis

The data distribution was analyzed via the Kolmogorov-Smirnov test. If the data were normally distributed with a p value > 0.05, a mean comparison test among treatment groups was conducted via *one-way ANOVA*. Pearson's correlation test was used, as the data were numerical, to determine the strength of the relationship between *Shh* expression and house gecko tail length. Linear regression analysis was also conducted to assess the effect of *Shh* expression on house gecko tail length. If the data were not normally distributed, comparisons were made via the *Kruskal-Wallis* test, and the *Spearman* correlation test was chosen for correlation analysis. The results were considered significant if the p value was < 0.05.

3. Results

3.1. Tail length measurement

The regeneration process of a house gecko's tail tissue is indicated by an increase in the length of the tail that has undergone autotomy. Measurements were taken of both the original and regenerated tails on days 1, 3, 7, 14, 21, and 30. The regenerated tail increased in length as the regeneration process progressed. Tail length was measured by placing the gecko on graph paper, as shown in Figure 1. Macroscopic observations revealed that on days 1 and 3, there was no visible increase in

the length of the regenerated tail. By day 7, the regenerated tail had grown and continued to lengthen on days 14, 21, and 30. The results of the measurements for the original and regenerated tails are shown in Figure 2.

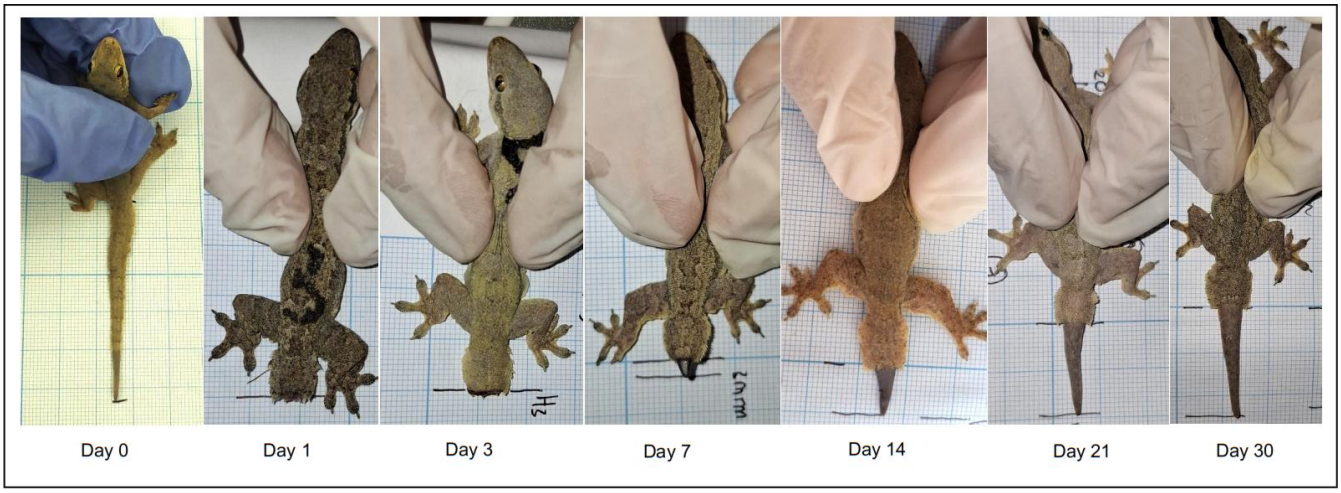

Figure 1 Procedure of house gecko (*H. platyurus*) tail length measurement.

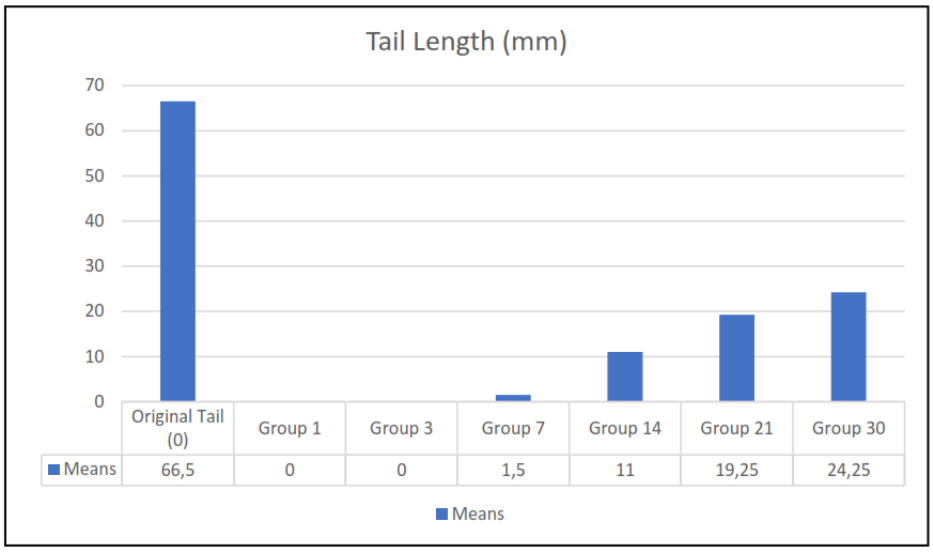

Figure 2 Tail length measurement of house gecko (*H. platyurus*) tail tissue.

The table shows that the tails grew slowly from day 1 to day 7 (the wound healing phase). The growth of the house gecko's tail began to increase rapidly from day 7 to day 21 (the blastema and regeneration phases) and then started to slow down from day 21 to day 30 (the maturation phase). Statistical analysis revealed that the data from the tail length measurements were normally distributed. The results can be analyzed via a parametric test. The mean comparison test via *one-way ANOVA* revealed a significant difference between the treatment groups ($p < 0.001$).

3.2. Histological analysis of tail tissue

The tail tissue of the house gecko is composed of highly complex components such as bone, cartilage, the spinal cord, ganglia, nerve fibers, skeletal muscle, adipose tissue, blood vessels, fibrous tissue, dermis, epidermis, and the keratin layer. With these complex components, the tail tissue of the house gecko can be used as an animal model to study the natural process of regeneration. The regeneration process of house gecko tail tissue provides different microscopic views of the original tail and the regenerated tail over different growth periods, as shown in Figures 3 and 4.

A histological view of a transverse section of the regenerated tail is shown in Figure 5, whereas a longitudinal section is displayed in Figure 6. These sections reveal various features as the regeneration process progresses. In the transverse section of the regenerated tail, no significant tissue growth was observed on days 1 and 3. During this period, tail regeneration occurs during the wound healing phase. Microscopically, on days 1 and 3, there was a cluster of erythrocytes indicating postautotomy bleeding, which began to decrease by day 3. Significant leukocyte infiltration is also observed in the tissue around the wound as an inflammatory response to autotomy.

A cluster of blastema cells begins to appear in the regenerated tail tissue on day 7, marking the transition of the regeneration process into the blastema phase. The blastema consists of stem cells in the tail tissue of the house gecko that proliferate and differentiate into mature cells. Numerous capillaries and nerve fibers are present to vascularize and innervate these blastema cells. In the central region, an ependymal canal surrounded by ependymal cells is found. Re-epithelialization was also visible at the site of the autotomy wound on day 7.

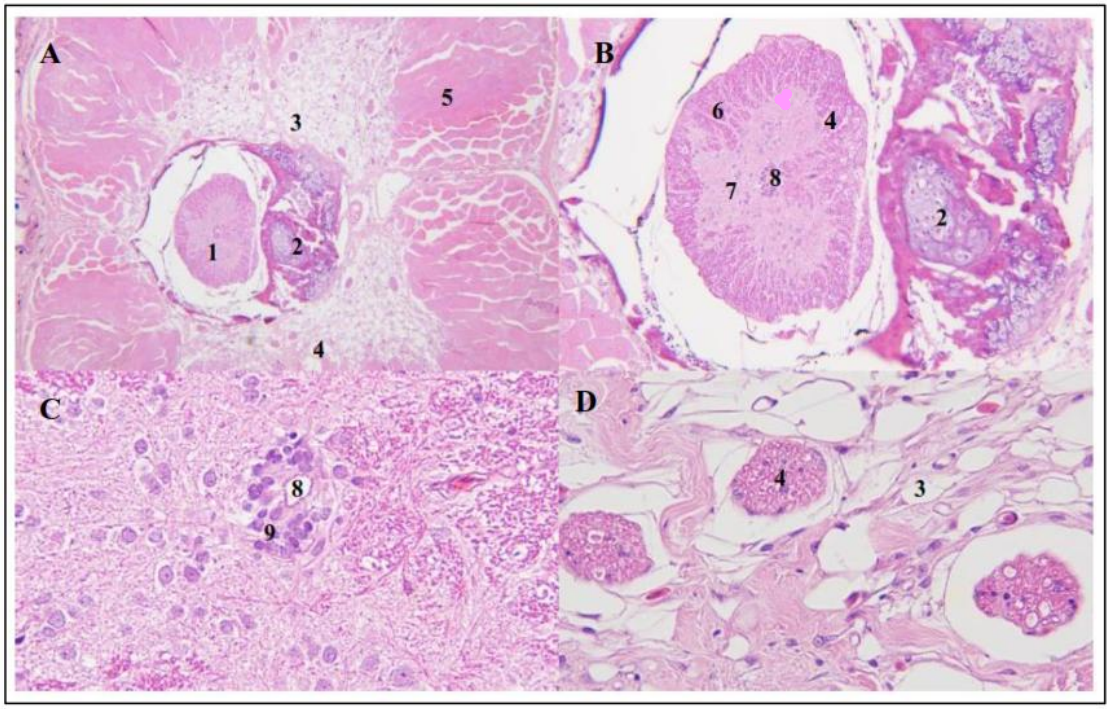

Figure 3 Microscopic view of transverse sections of original tail tissue (Group 0). (A) View of the spinal cord and surrounding tissue at 4x10 magnification. (B) Spinal cord and vertebral body at 10x10 magnification. (C) Gray matter with the central canal surrounded by ependymal cells at 40x10 magnification. (D) Transversesection of nerve fibers at 40x10 magnification. Key: 1. Spinal cord, 2. Vertebral body, 3. Adipose tissue, 4. Nerve fibers, 5. Skeletal muscle tissue, 6. White matter, 7. Gray matter, 8. Central canal, 9. Ependymal cells around the central canal.

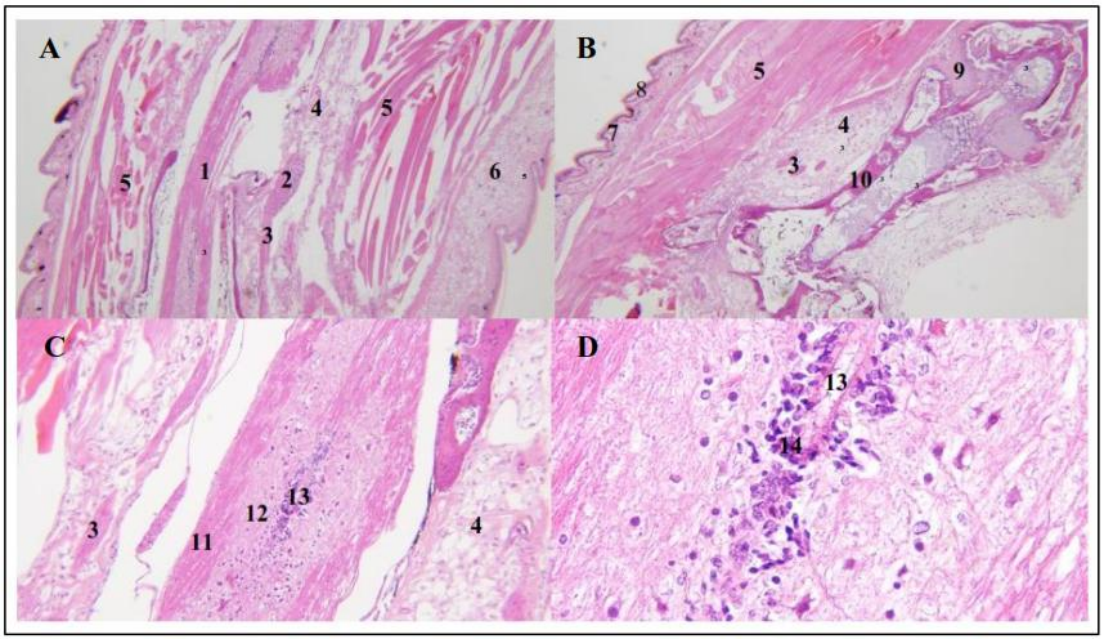

Figure 4 Microscopic view of longitudinal sections of original tail tissue (Group 0). (A) Longitudinal section of the spinal cord and surrounding tissue at 4x10 magnification, (B) vertebral body and intervertebral disc at 4x10 magnification, (C) spinal cord and nerve fibers at 10x10 magnification, (D) gray matter with the central canal surrounded by ependymal cells at 40x10 magnification. Key: 1. Spinal cord, 2. Ganglion, 3. Nerve fibers, 4. Adipose tissue, 5. Skeletal muscle tissue, 6. Subcutaneous adipose tissue, 7. Dermis, 8. Epidermis, 9. Intervertebral disc, 10. Vertebral body, 11. White matter, 12. Gray matter, 13. Central canal, 14. Ependymal cells around the central canal.

The blastema cells differentiated into mature cells in the regenerated tail tissue on day 14. This phase is referred to as the regeneration phase. Microscopically, a complex tissue structure is visible, with an ependymal canal surrounded by ependymal cells and *cauda equina* in the central area. The vertebral body, which is composed of cartilage tissue, encircles the ependymal canal. Around the vertebral body, adipose tissue is present, with numerous capillaries and nerve fibers between the adipocytes. A large amount of connective tissue was also observed in the regenerating tail on day 14. Skeletal muscle tissue has formed along the regenerated tail. The epidermis and dermis have fully developed, with a keratin layer on the surface.

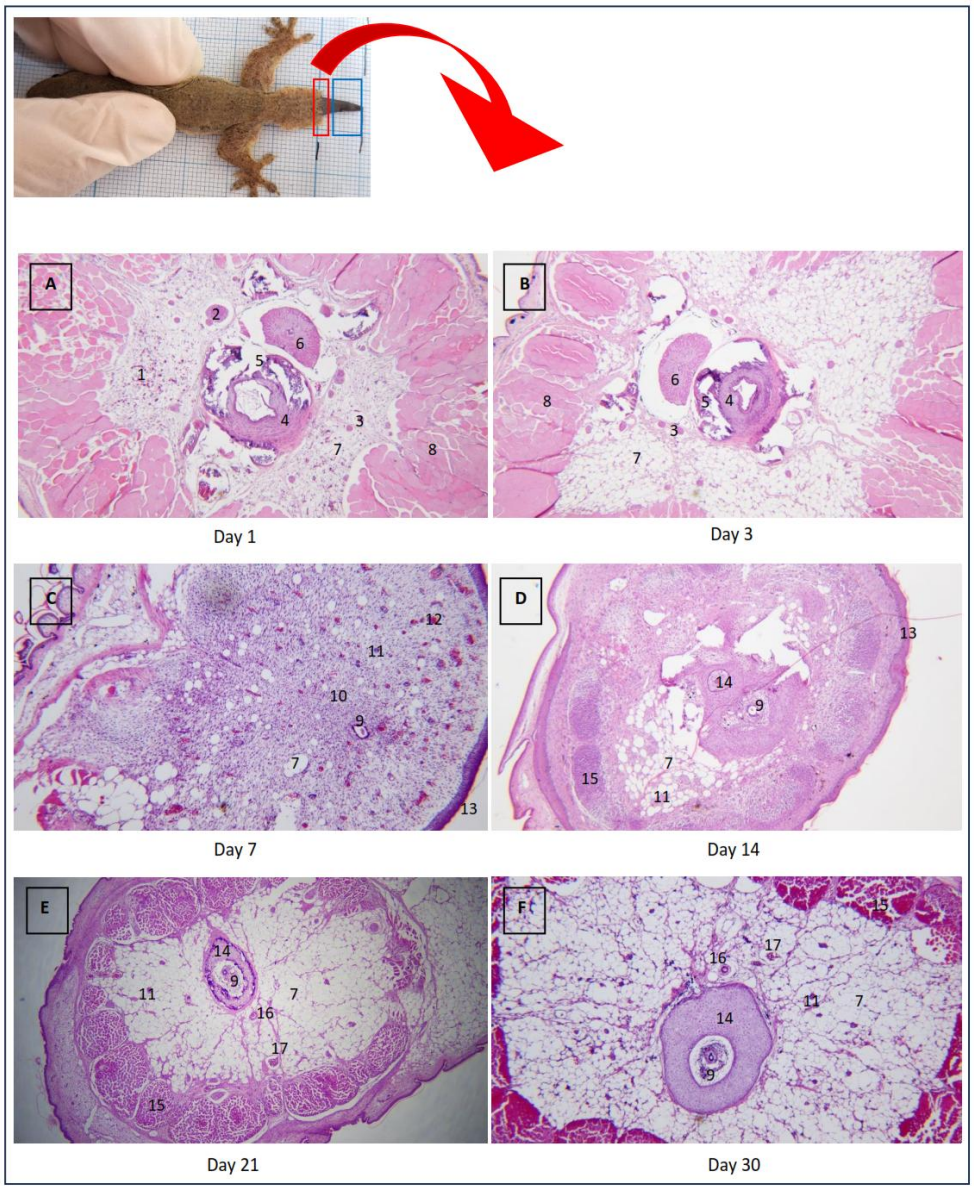

Figure 5 Microscopic view of transverse sections of regenerated tail tissue on days 1, 3, 7, 14, 21, and 30. (A) Transverse section of regenerated tail tissue on day 1 showing no histological changes. A cluster of erythrocytes indicates postautotomy bleeding, with leukocyte infiltration visible around the wound tissue. (B) The transverse section of the regenerated tail tissue on day 3 also shows no histological changes. Erythrocytes are beginning to decrease, but leukocyte infiltration is still prevalent. (C) The transverse section of the regenerated tail tissue on day 7 shows a cluster of blastema cells with numerous capillaries and nerve fibers. In the central part, an ependymal canal surrounded by ependymal cells is visible. (D) The transverse section of the regenerated tail tissue on day 14 provides a clearer histological view, where the blastema has differentiated into mature cells according to their destined functions. The ependymal canal is located centrally and is surrounded by ependymal cells and nerve fibers (cauda equina). The ependymal canal is situated in the center of the vertebral body and consists of cartilage. (E) and (F) Transverse sections of regenerated tail tissue on days 21 and 30 showing a more complex histological structure resembling the original tail. Key: 1. A cluster of erythrocytes and leukocyte infiltration; 2. Peripheral nerve ganglion, 3. Nerve fibers, 4. Intervertebral disc, 5. Vertebral body, 6. Spinal cord, 7. Adipose tissue, 8. Skeletal muscle, 9. pendymal canal with surrounding ependymal cells, 10. Blastema cells, 11. Nerve fibers in the blastema cluster, 12. Capillaries, 13. Epidermis and dermis with a keratin layer on the surface; 14. Regenerated vertebral body, 15. Regenerated skeletal muscle, 16. Caudal artery, 17. Caudal vein.

The microscopic view on days 21 and 30 revealed increasingly complex and differentiated tissue resembling the original tail. In this regenerated tail, the spinal medulla does not regenerate. The spinal cord is replaced by an ependymal canal surrounded by ependymal cells and the cauda equina. At this stage, the regeneration process has entered the maturation phase.

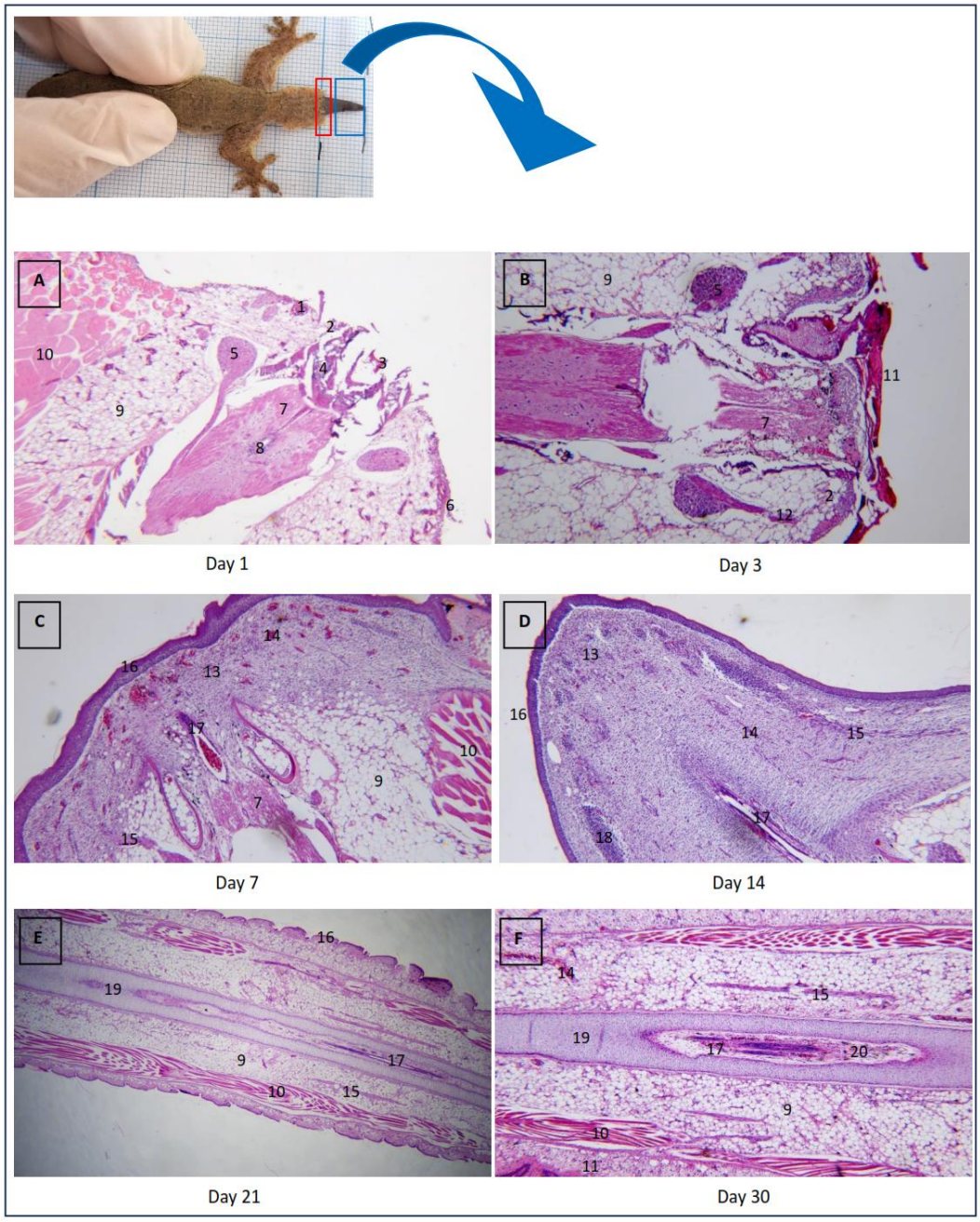

Figure 6 Microscopic view of longitudinal sections of regenerated tail tissue on days 1, 3, 7, 14, 21, and 30. (A) Longitudinal section of the regenerated tail on day 1 showing no tail growth. The tail tissue appears peeled, with clusters of erythrocytes and leukocyte infiltration at the autotomy wound site. (B) Longitudinal section of regenerated tail on day 3 reveals re-epithelialization in the wound area, indicating the wound healing process. (C) Longitudinal section on day 7 displays clusters of blastema cells in the distal tail region. Numerous capillaries and nerve fibers are observed among blastema cells. The ependymal canal also grows caudally in the central tail tissue. (D) Longitudinal section on day 14 shows significant tail elongation, with an increased concentration of blastema cells and the presence of skeletal muscle progenitor cells. More nerve fibers and capillaries are visible among the blastema cell clusters. (E) and (F) Longitudinal sections on days 21 and 30 show tail growth that increasingly resembles the original tail structure. The spinal cord is replaced by the ependymal canal, and the formed vertebral bodies consist of continuous cartilage. Key: 1. Erythrocyte clusters, 2. Leukocyte infiltration, 3. Detached tissue section, 4. Vertebral body, 5. Peripheral nerve ganglion, 6. Keratin layer, 7. Spinal cord, 8. Central canal, 9. Adipose tissue, 10. Skeletal muscle tissue, 11. Wound re-epithelialization, 12. Nerve fibers, 13. Blastema cells, 14. Capillaries, 15. Nerve fibers of regenerated tail, 16. Epidermis and dermis, 17. Ependymal canal, 18. Skeletal muscle progenitor cells, 19. Discontinuous cartilage, 20. Cauda equina.

In the longitudinal section, the regeneration process can be observed from the base to the tip of the regenerated tail. The first phase of regeneration is the wound healing phase. On day 1, no tissue growth was visible in the cross-sectional tissue. Part of the tail tissue appears detached because of the autotomy process. There is a cluster of erythrocytes indicating bleeding in the wound area. Significant infiltration of leukocytes is also found at the wound site as an inflammatory response following injury. By day 3, the wound healing process was evident, with re-epithelialization at the site of autotomy. Substantial infiltration of leukocytes remains visible in this area. In this phase, nerve fibers and capillaries from the proximal tissue begin to grow toward the wound area.

The transverse tissue section of the regenerated tail on day 7 shows complete re-epithelialization of the distal tail, as indicated by the formation of an epidermal layer encasing the wound site. Numerous blastemal cells are visible and are surrounded by capillaries and nerve fibers. In the central region, the ependymal canal extends toward the distal end of the regenerating tail. These blastemal cells proliferate and differentiate into mature cells. By day 7, the tail tissue had entered the blastema phase, with observable tissue growth both microscopically and macroscopically.

By day 14, the regenerated tail tissue appeared more elongated. An increased concentration of blastemal cells is visible, along with numerous muscle progenitor cells around the tail tissue. Extending nerve fibers and a growing network of capillaries are evident among the blastema. The ependymal canal continues centrally toward the caudal region of the tail tissue. The chondroblast progenitor cells surrounding the ependymal canal are visible and eventually form cartilage.

Transverse sections of tail tissue on days 21 and 30 revealed that the regenerated tail increasingly resembled the structure of the original tail tissue. Microscopic examination reveals differences in the regenerative process: while the spinal medulla does not regenerate caudally, the ependymal canal surrounded by ependymal cells regenerates and extends caudally. This ependymal canal is also encircled by the surrounding cauda equina. The structure of the vertebral bodies also changes. In the original tail, the vertebral bodies consisted of bone segments connected by intervertebral discs. In the regenerated tail, the vertebral bodies are composed of continuous cartilage extending caudally, enclosing the ependymal canal within the vertebral column. The tissues surrounding the vertebral bodies, including adipose, fibrous, skeletal muscle, blood vessel, subcutaneous, dermis, and epidermis, continue to resemble the histology of the original tail tissue.

3.3. Immunohistochemical analysis of Shh expression and distribution

IHC staining revealed that the Shh protein is expressed in both the original and regenerated tail tissues of the common house gecko. However, differences in expression density were observed between the groups, as shown in Figure 7. Shh protein expression in regenerated tail tissue progressively increased from day 1 to day 14 and stabilized until day 21. A subsequent decrease in *Shh* expression was observed from day 21 to day 30. The positive control tissue used in this study was mouse kidney tissue, in accordance with the datasheet for the rabbit anti-Shh primary antibody (NBP2-22139 Sonic Hedgehog/*Shh* Antibody-BSA Free) used in this study. Positive IHC results revealed that the nuclei and cytoplasm of the mouse kidney cells were positive. The negative control for the IHC staining was the original tail tissue of the common house gecko. IHC staining revealed that the *Shh* protein was also expressed in the original tail. Positive staining in the original tail was observed in epithelial cells, fibroblasts, adipocytes, neurons, chondroblasts, Schwann cells, and skeletal muscle cells, as shown in Figure 8. Moreover, positive staining in the regenerated tail was distributed in blastema cells, epithelial cells, fibroblasts, adipocytes, skeletal muscle progenitor cells, skeletal muscle cells, neurons in the proximal spinal cord, chondroblasts, Schwann cells, ependymal cells, and endothelial cells, as shown in Figure 9.

A semiquantitative analysis of *Shh* protein expression was conducted by measuring the density of the tissue area with positive staining. The area density measurement was performed via *ImageJ* software. The results for the area density with positive Shh expression are shown in Figure 10. Immunohistochemical staining revealed that the Shh protein remained expressed in the original tail tissue of adult house geckos. One day postautotomy, an increase in Shh expression is observed. This increase continues to intensify up to day 14 (blastema phase) and is sustained through week 21 (regeneration phase), followed by a rapid decline from day 21 to day 30 (maturation phase).

3.4. Statistical analysis

Statistical analysis was conducted on the obtained numerical data. The *Kolmogorov-Smirnov* test indicated a normal data distribution, allowing for parametric analysis. *One-way ANOVA* for the mean comparison test revealed a significant difference among the treatment groups (p<0.001). A *Pearson* correlation test was then applied to assess the relationship between Shh expression and house gecko tail length. The *Pearson* correlation results revealed a strong positive correlation between *Shh* expression and regenerated tail length from day 1 to day 14 (R=0.818; p<0.001). Additionally, a strong negative correlation was observed between *Shh* expression and regenerating tail length from day 21 to day 30 (R=-0.852; p<0.001). Linear regression analysis was also performed in this study. The linear regression results revealed that *Shh* expression accounts for 67% of the variation in regenerating tail length from day 1 to day 14 (R^2=0.67; p<0.001), with the equation Y = -5.654 + 0.340X (where Y represents regenerating tail length and X represents *Shh* expression). Linier regression analysis further revealed that *Shh* expression accounts for 72.6% of the variation in regenerating tail length from day 21 to day 30 (R^2=0.726;

p<0.001), with the following equation: Y = 48.593-0.862X (where Y represents regenerating tail length and X represents *Shh* expression).

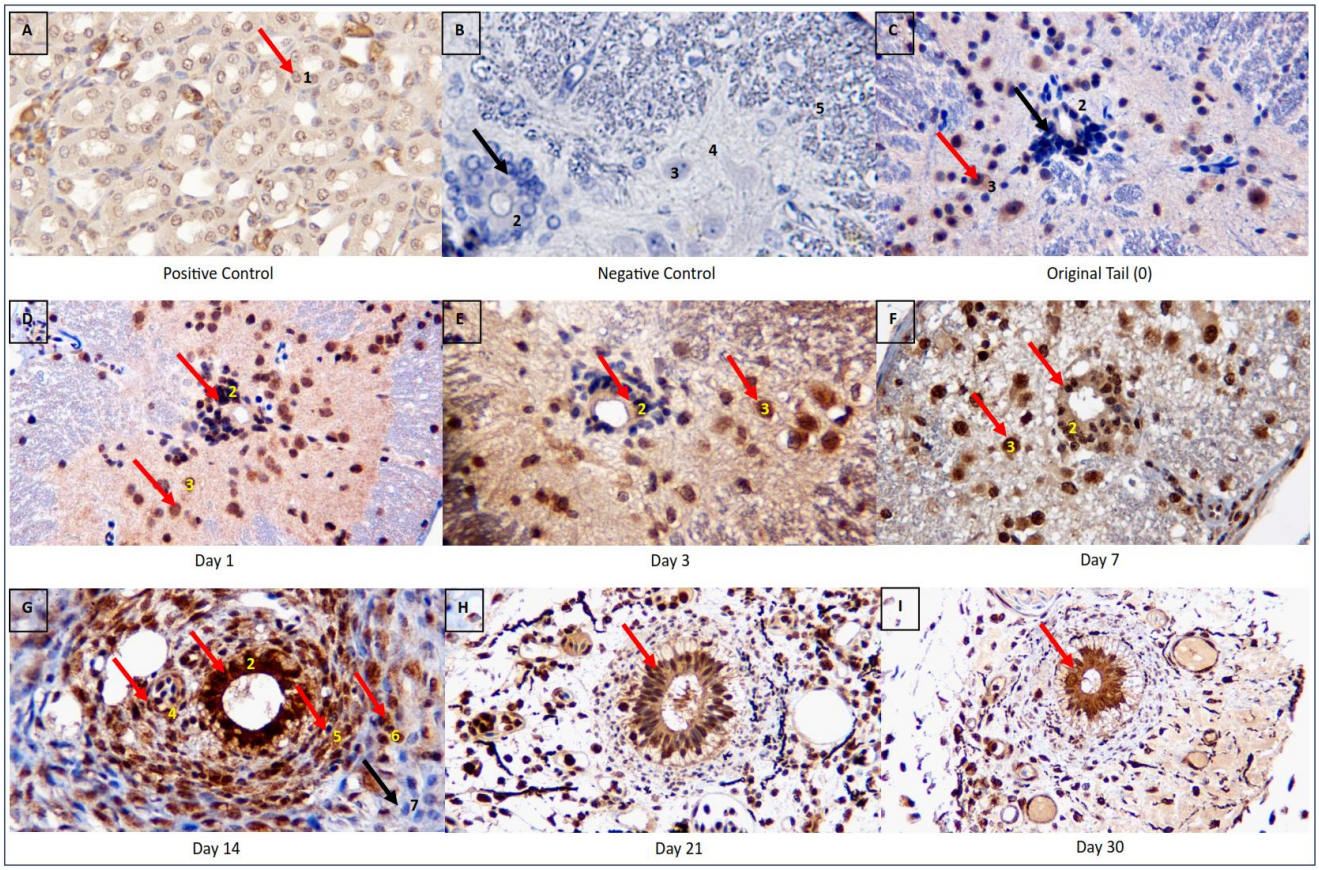

Figure 7 Immunohistochemistry (IHC) analysis of the *Shh* protein at 40x10 magnification: (A) IHC analysis of the *Shh* protein in the positive control using mouse kidney tissue sections, with the red arrowhead indicating *Shh* protein expression in the nuclei and cytoplasm of tubular cells (darker brown), (B) IHC analysis of the *Shh* protein in the negative control using original tail tissue (blue color), (C) IHC analysis of the *Shh* protein in the spinal cord of the original tail of a house gecko. The red arrow indicates positively stained cells (brown), indicating neurons in the gray matter, whereas the blue arrow indicates negatively stained cells (blue), indicating ependymal cells surrounding the central canal. (D) IHC analysis of the *Shh* protein in the spinal cord of the regenerated tail on day 1. Positive staining begins to appear in ependymal cells, with increasing density in gray matter. (E) IHC analysis of the *Shh* protein in the spinal cord of the regenerated tail on day 3. Positive staining increased in numerous cells extending into the white matter. (F) IHC analysis of the *Shh* protein in the spinal cord of the regenerated tail on day 7. Almost all the cells and tissues within the spinal cord showed positive staining. (G) IHC analysis of the *Shh* protein in the ependymal canal of the regenerated tail on day 14. IHC staining on day 14 revealed intense staining in ependymal cells surrounding the ependymal canal, surrounding fibroblasts, and actively proliferating chondroblasts in the vertebral body. Additionally, endothelial cells forming the anterior spinal artery and vein were also positively stained. (H) IHC analysis of the *Shh* protein in the ependymal canal of the regenerated tail on day 21. Positive staining remained visible, although with a slight decrease in density. (I) IHC analysis of the *Shh* protein in the ependymal canal of the regenerated tail on day 30. A decrease in the density of positive IHC staining was observed in the regenerated tail tissue. Key: 1. Mouse kidney tubular cells, 2. Ependymal cells, 3. Neurons, 4. Endothelial cells surrounding the anterior spinal artery, 5. Fibroblasts, 6. Chondroblasts, 7. Chondrocytes.

4. Discussion

These results indicate that the morphogen *Shh* is expressed in both the original and regenerated tails. However, the density of *Shh* expression in the original tail is significantly lower than that in the regenerated tail. *Shh* expression in normal tissue plays a key role in tissue homeostasis. Following tissue injury, *Shh* expression gradually increases. *Shh* is crucial for cell survival, differentiation, and proliferation, thereby supporting tissue regeneration.

Activation of the *Shh* signaling pathway occurs through two mechanisms: canonical and noncanonical signaling. Canonical *Shh* signaling takes place when the *Shh* glycoprotein binds to and inactivates the 12-transmembrane protein Patched (*Ptch1*). In the absence of *Shh* binding, *Ptch1* inhibits the activation of the 7-transmembrane protein Smoothened (*Smo*); thus, the binding of *Shh* to *Ptch1* regulates the activation of *Smo*, leading to the downstream *Shh* signaling cascade (Bangs & Anderson, 2017; Carballo et al., 2018).

The *Shh* signaling cascade induces the translocation of Gli family proteins to the nucleus, initiating the transcription of numerous target genes. The three *Gli* family proteins (*Gli*1, *Gli*2, and *Gli3*) are *Shh*-dependent zinc-finger transcription factors.

*Gli*1 functions as a full-length transcriptional activator, whereas *Gli*2 and *Gli*3 can act as either positive or negative regulators (Carballo et al., 2018). *Gli*-targeted genes regulate cell differentiation, proliferation, and survival. *Gli*1 activates proteins such as *Shh, Ptch*, and *Gli*2. *Gli*2, in turn, regulates cell cycle-related proteins, including the proto-oncogene *N-myc* and *cyclin D*. *Shh* also plays a role in cell proliferation, differentiation, and migration through cross-talk with other signaling pathways, such as the *MAPK/ERK, PI3K/AKT/*m*TOR, EGFR*, and *NOTCH* pathways (Choudhry et al., 2014).

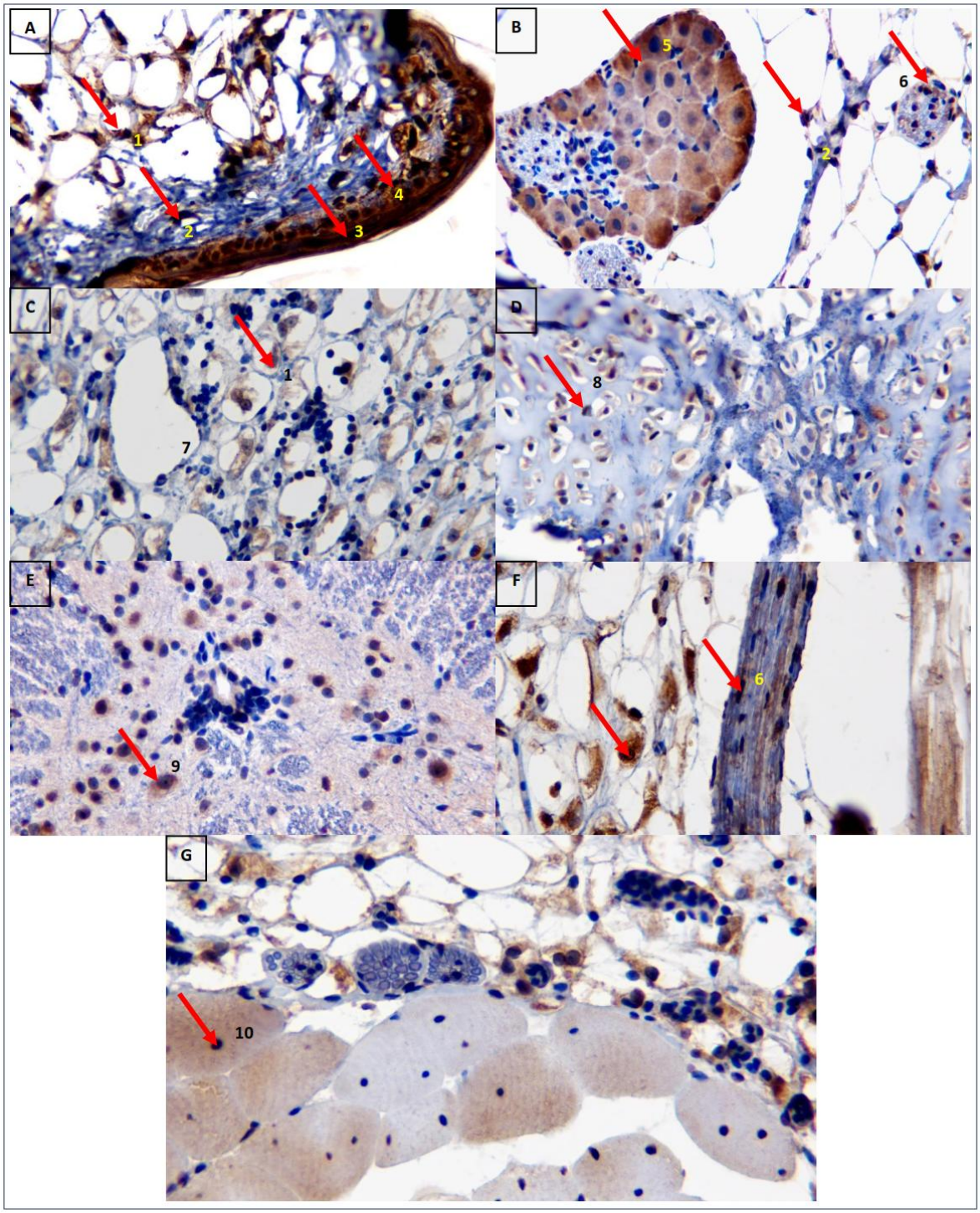

Figure 8 Distribution of *Shh* expression in the original tail of the house gecko (*H. platyurus*) at 40x10 magnification. (A) Positive staining observed in epithelial cells, fibroblasts, and adipocytes, as indicated by the red arrow; (B) positive staining observed in ganglion cells, fibroblasts, and Schwann/fibroblasts forming the myelin sheath; (C) positive staining observed in actively proliferating adipocytes; (D) positive staining observed in actively proliferating chondroblasts; (E) positive staining observed in neurons within the gray matter of the spinal cord; (F) positive staining observed in Schwann/fibroblasts forming the myelin sheath in longitudinal tissue sections; (G) positive staining observed in skeletal muscle cells. Key: 1. Adipocytes, 2. Fibroblasts, 3. Epidermal layer, 4. Dermal layer, 5. Ganglion cells, 6. Schwann cells, 7. Endothelial cells, 8. Chondroblasts, 9. Neuron, 10. Skeletal muscle cells.

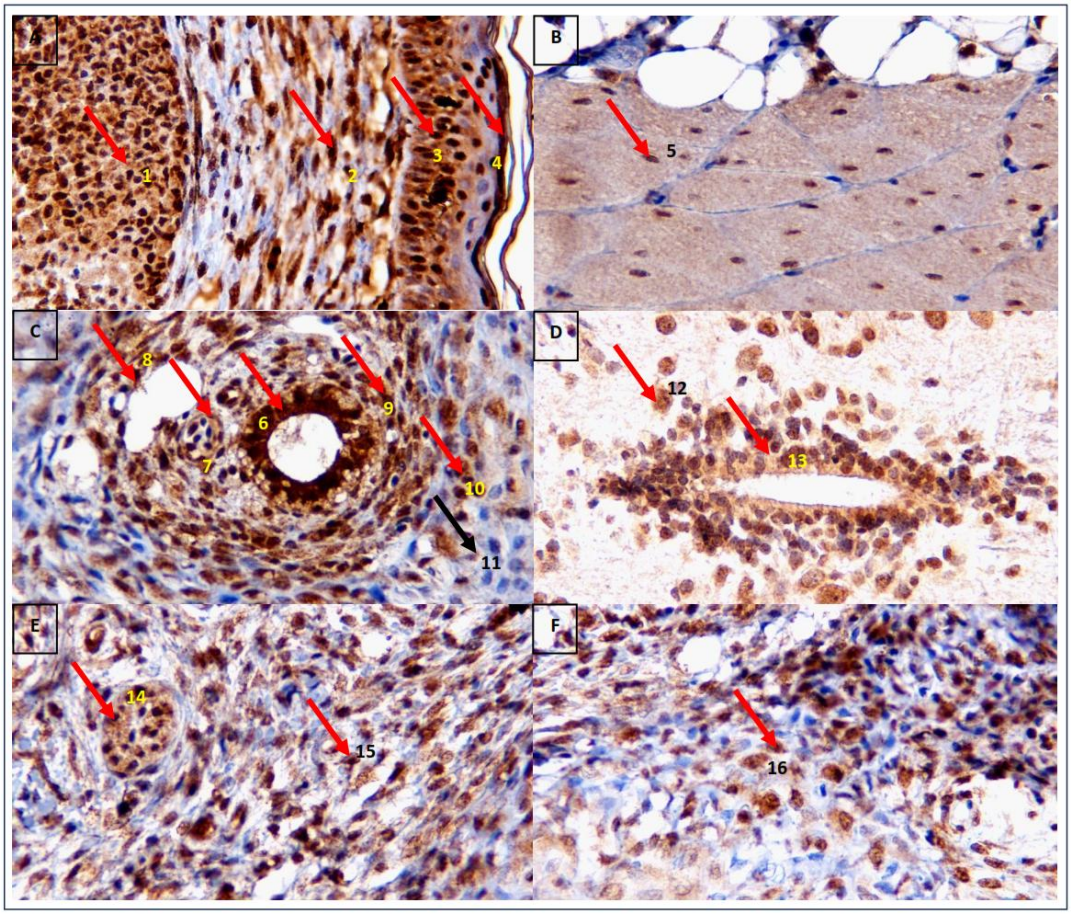

Figure 9 Distribution of *Shh* expression in the regenerated tail of the house gecko (*H. platyurus*) at 40x10 magnification. (A) Positive staining observed in skeletal muscle progenitor cells, fibroblasts, and epithelial cells in the epidermal and dermal layers, as indicated by the red arrow. (B) Positive staining observed in skeletal muscle cells. (C) Positive staining observed in ependymal cells surrounding the ependymal canal, endothelial cells forming anterior spinal artery and vein, fibroblasts, and actively proliferating chondroblasts. (D) Positive staining observed in neurons within the gray matter in the proximal spinal cord. (E) Positive staining observed in fibroblasts, adipocytes, and Schwann/fibroblasts cells forming the myelin sheath. (F) Positive staining observed in blastema cells. Key: 1. Muscle progenitor cells, 2. Fibroblasts, 3. Dermal layer, 4. Epidermal layer, 5. Skeletal muscle cells, 6. Ependymal cells, 7. Endothelial cells around the anterior spinal artery; 8. Endothelial cells around the anterior spinal vein; 9. Fibroblasts, 10. Actively proliferating chondroblasts, 11. Chondrocytes, 12. Neurons, 13. Ependymal cells surrounding the central canal in the proximal spinal cord; 14. Schwann cells that form the myelin sheath; 15. Adipocytes, 16. Clusters of blastemas.

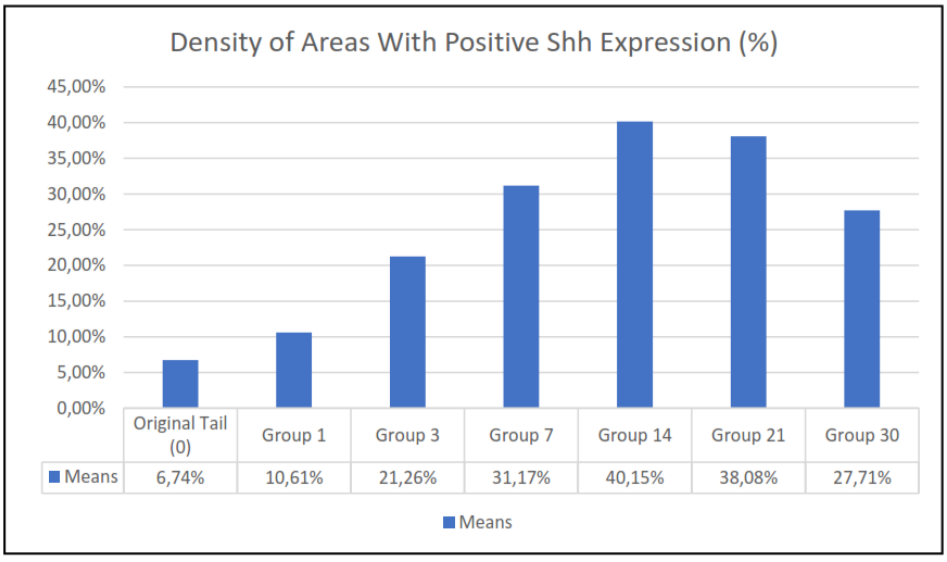

Figure 10 Density of areas with positive Shh expression (%) in both original and regenerated tails across the treatment groups.

The noncanonical *Shh* signaling pathway operates through *Gli*-independent mechanisms and is divided into two types. Type I is downstream of *Smo* and modulates Ca^{2+} and the actin cytoskeleton, whereas type II is independent of *Smo* and promotes cell proliferation and survival. Noncanonical signaling can regulate chemotaxis and cell migration through actin rearrangement. Additionally, this pathway can stimulate cell proliferation via calcium-induced extracellular signal-regulated kinase (*ERK*) activation and *Src* family kinases (Mastrangelo & Milani, 2018).

The density of *Shh* expression during the regeneration process corresponds to the stages of tail tissue regeneration following autotomy. Lizard tail regeneration occurs in several stages following autotomy (Novianti et al., 2019). The initial wound healing phase (days 0–10) involves blood clotting, an inflammatory response, and macrophage activation for debris clearance and wound preparation. Re-epithelialization also begins during this phase. The blastema phase (days 10–15) follows, with pluripotent blastema cells accumulating at the wound site, where they migrate, proliferate, and differentiate into various cell types guided by signaling pathways. The regeneration phase (days 15–25) involves tail elongation, as differentiated cells, such as ependymal cells, chondroblasts, adipocytes, fibroblasts, endothelial cells, muscle cells, Schwann cells, and epithelial cells, form and proliferate, supporting tail growth. Finally, in the maturation phase (after day 25), the regenerated tail tissue resembles and functions similarly to the original tail.

The results of this study indicate that *Shh* expression increases from day 1 postautotomy due to tissue injury. Research on glioblastoma tumors has shown that tumor cells secrete inflammatory cytokines, growth factors, and other proteins that can induce the activation of the *Shh* signaling pathway (Sigafoos et al., 2021). Similarly, during tissue injury, high levels of inflammatory cytokines and growth factors are produced to support regeneration. Autotomy of the tail tissue of house geckos leads to extensive tissue damage, prompting damaged tissues to synthesize specific growth factors that promote cell survival and regeneration. On day 7, the density of *Shh* expression increased progressively, peaking on day 14. This corresponds with the regeneration process of the house gecko's tail, which enters the blastema phase. During this phase, rapid proliferation and differentiation of blastema cells occur, forming new differentiated cells that then proceed into the regeneration phase. The density of *Shh* expression begins to decrease from day 21 to day 30 as the process enters the maturation phase, when tail comprises complex tissues, including neural tissue, bone, cartilage, muscle, connective tissue, adipose tissue, blood vessels, and epithelial cells in both the epidermis and dermis (Alibardi, 2010). *Shh* expression in the original tail tissue of the house gecko is prominently observed in epithelial cells, neurons, ganglion cells, fibroblasts, and adipocytes. Chondroblasts and Schwann cells show moderate positive staining, whereas skeletal muscle cells show weak positive staining. In the regenerated tail of house geckos, expression levels across all tissues, including blastema cells, which are pluripotent stem cells found in the lizard tail, and ependymal cells surrounding the ependymal tube, which are continuations of the central canal in the regenerated tail, increase following autotomy. Furthermore, endothelial cells in blood vessels also express *Shh* during angiogenesis.

Hh signaling is essential for skin development; the loss of *Shh* expression is associated with disruptions in follicle development, keratinocyte proliferation, and dermal papilla maturation. In adult tissue, *Hh* expression persists to maintain skin homeostasis. In the skin of adult tissue, *Shh* is detected in stem cell and progenitor cell clusters essential for hair growth and skin regeneration through fibroblast proliferation (Lau et al., 2022).

During embryonic development, *Hh* signaling plays a crucial role in nervous system development. *Hh* interacts with receptors, coreceptors, and proteins that activate both canonical and noncanonical signaling pathways, regulating intercellular interactions that influence neural development. *Shh* specifically activates proliferative and morphogenic mechanisms in neural stem and progenitor cells, especially in motor neurons, neuronal differentiation, axonal pathfinding, and synapse formation (Belgacem et al., 2016). In adult tissue, Shh, along with the *Ptch1* receptor complex and *Smo*, is expressed in adult neural tissue, primarily in the cytoplasm. *Shh* levels increase in response to peripheral nerve injury, both in the dorsal root ganglion and the proximal segment of the injury (Martinez et al., 2015).

Shh signaling plays an essential role in fibroblast proliferation, particularly in wound healing and tissue regeneration processes. In adult tissues, *Shh* stimulates fibroblast activity by interacting with its receptor complex, comprising *Ptch1* and *Smo*, which in turn activates downstream signaling pathways. This activation promotes fibroblast proliferation, differentiation, and migration to the wound site, contributing to the formation of new extracellular matrix components and supporting the repair of damaged tissues (Frech et al., 2022). The *Hh* signaling pathway is also involved in adipogenesis in adipocytes (Kyung et al., 2024).

Shh signaling plays a significant role in chondrogenesis, particularly in limb and tail regeneration in lizards. *Shh* signaling influences the behavior of mesenchymal stem cells, which are crucial for cartilage formation. During tail regeneration, *Shh* helps establish the correct spatial pattern of the developing cartilage. It is crucial for defining the anterior-posterior axis, ensuring that the regenerated tail has the proper shape and structure (Lozito et al., 2021; Vonk et al., 2023).

Following autotomy, the tail tissue in house geckos experiences injury and enters hypoxic conditions, resulting in an increase in hypoxia-inducible factor-1α (*HIF-1α*) (Novianti et al., 2019). The *Hh* signaling pathway can be detected in adult tissues under both physiological and pathological conditions, such as ischemia. *Hh* plays a role in the regeneration of ischemic tissues through angiogenesis. Upregulation of *Hh* can be observed in ischemic skeletal muscle, which may be mediated by the

presence of *HIF-1α*. Sonic Hedgehog (*Shh*) responds to angiogenic growth factors produced by fibroblasts and stimulates the proliferation, migration, and survival of endothelial cells (ECs) (Straface et al., 2009).

Shh signaling also plays an essential role in the development and regeneration of skeletal muscle cells. *Shh* is crucial during embryonic development, particularly in the formation of somites, which give rise to skeletal muscle. *Shh* signaling helps establish muscle progenitor cells in somites and promotes their differentiation into myoblasts (muscle precursor cells) (Piccioni et al., 2014). In response to muscle injury, *Shh* signaling is reactivated to support the regeneration of damaged muscle tissue. Satellite cells, which are adult muscle stem cells, are activated upon injury. Shh signaling enhances their proliferation and differentiation into mature muscle fibers (Straface et al., 2009).

In the regenerated tail tissue of house geckos, ependymal cells surrounding the ependymal tube, which is a continuation of the central canal of the spinal cord, strongly express *Shh*. In response to injury or pathological conditions, ependymal cells can reactivate the expression of *Shh.* The *Shh* expressed in lizard tail tissue is responsible for cartilage formation during regeneration of the tail.

5. Conclusions

The *Shh* protein is expressed in both original tail tissue and regenerated tail tissue. The *Shh* signaling pathway functions to maintain tissue homeostasis in adult tissues. Following autotomy, *Shh* expression increases in response to injury, activating the proliferation, migration, and differentiation of blastema cells to form differentiated cells that support the regeneration process. *Shh* protein expression increases following injury, peaking on day 14. Shh expression persists until day 21, after which it begins to decrease until day 30. Shh is expressed in numerous cells within both the original and regenerated tail tissues of the house gecko. It is expressed not only in ependymal cells surrounding the ependymal tube but also in various tissues, including nerve tissue, cartilage, connective tissue, adipose tissue, muscle, blood vessels, and the epithelium in both the epidermal and dermal layers, as well as in blastema cells, which are pluripotent progenitor cells located in the tail tissue of house geckos.

Acknowledgment

The authors would like to thank the Ministry of Education, Culture, Research, and Technology for the research grant and Universitas Sultan Ageng Tirtayasa for the Study Assignment Scholarship. The authors also acknowledge the facilities, scientific and technical support from Zoology Characterization Laboratories, National Research and Innovation Agency through E- Layanan Sains, Badan Riset dan Inovasi Nasional.

Ethical considerations

The research protocol was reviewed and approved by the Faculty of Medicine of the University of Indonesia's Research Ethics Committee (number: KET-349/UN2.F1/ETIK/PPM.00.02/2024).

Conflict of interest

The authors declare that they have no conflicts of interest.

Funding

This research was funded by a grant from the State University Operational Assistance Program, Research Program, Fiscal Year 2024, provided by the Directorate of Research, Technology, and Community Service, Directorate General of Higher Education, Research, and Technology, Ministry of Education, Culture, Research, and Technology, with grant number: NKB-863/UN2.RST/HKP.05.00/2024.

References

Alibardi, L. (2010). Morphological and cellular aspects of tail and limb regeneration in lizards: A model system with implications for tissue regeneration in mammals. In H. W. Korf, F. Beck, F. Clasca, M. Frotscher, D. Haines, N. Hirokawa, Z. Kmiec, E. Marani, R. Putz, & J. P. Timmermans (Eds.), *Advances in anatomy, embryology and cell biology*. Springer. http://www.springer.com/series/102

Bangs, F., & Anderson, K. V. (2017). Primary Cilia and Mammalian Hedgehog Signaling. *Cold Spring Harbor Perspectives in Biology*, *9*(5). https://doi.org/10.1101/cshperspect.a028175

Barresi, M. J. F., & Gilbert, S. F. (2020). *Developmental Biology* (12th ed.). Oxford University Press.

Belgacem, Y. H., Hamilton, A. M., Shim, S., Spencer, K. A., & Borodinsky, L. N. (2016). The many hats of Sonic hedgehog signaling in nervous system development and disease. In *Journal of Developmental Biology* (Vol. 4, Issue 4). MDPI Multidisciplinary Digital Publishing Institute. https://doi.org/10.3390/jdb4040035

Carballo, G. B., Honorato, J. R., De Lopes, G. P. F., & Spohr, T. C. L. D. S. E. (2018). A highlight on Sonic hedgehog pathway. In *Cell Communication and Signaling* (Vol. 16, Issue 1). BioMed Central Ltd. https://doi.org/10.1186/s12964-018-0220-7

Choudhry, Z., Rikani, A. A., Choudhry, A. M., Tariq, S., Zakaria, F., Asghar, M. W., Sarfraz, M. K., Haider, K., Shafiq, A. A., & Mobassarah, N. J. (2014). Sonic hedgehog signalling pathway: a complex network. *Annals of Neurosciences*, *21*(1). https://doi.org/10.5214/ans.0972.7531.210109

Dzobo, K., Thomford, N. E., Senthebane, D. A., Shipanga, H., Rowe, A., Dandara, C., Pillay, M., & Motaung, K. S. C. M. (2018). Advances in Regenerative Medicine and Tissue Engineering: Innovation and Transformation of Medicine. *Stem Cells International*, *2018*, 1–24. https://doi.org/10.1155/2018/2495848

Frech, S., Forsthuber, A., Korosec, A., Lipp, K., Kozumov, V., & Lichtenberger, B. M. (2022). Hedgehog Signaling in Papillary Fibroblasts Is Essential for Hair Follicle Regeneration during Wound Healing. *The Journal of Investigative Dermatology*, *142*(6), 1737-1748.e5. https://doi.org/10.1016/j.jid.2021.11.026

Goldman, J. A., & Poss, K. D. (2020). Gene regulatory programmes of tissue regeneration. In *Nature Reviews Genetics* (Vol. 21, Issue 9, pp. 511–525). Nature Research. https://doi.org/10.1038/s41576-020-0239-7

Kyung, D. S., Lee, E., Chae, S., Son, Y., Moon, Y.-J., Hwang, D., Kim, J. K., Lee, Y.-H., & Seong, J. K. (2024). Single-cell transcriptomic analysis reveals dynamic activation of cellular signaling pathways regulating beige adipogenesis. *Experimental & Molecular Medicine*, *56*(10), 2309–2322. https://doi.org/10.1038/s12276-024-01252-9

Lau, C. I., Yánez, D. C., Papaioannou, E., Ross, S., & Crompton, T. (2022). Sonic Hedgehog signalling in the regulation of barrier tissue homeostasis and inflammation. *FEBS Journal*, *289*(24), 8050–8061. https://doi.org/10.1111/febs.16222

Lozito, T. P., & Tuan, R. S. (2017). Lizard tail regeneration as an instructive model of enhanced healing capabilities in an adult amniote. *Connective Tissue Research*, *58*(2), 145–154. https://doi.org/10.1080/03008207.2016.1215444

Lozito, T. P., Londono, R., Sun, A. X., & Hudnall, M. L. (2021). Introducing dorsoventral patterning in adult regenerating lizard tails with gene-edited embryonic neural stem cells. *Nature Communications*, *12*(1). https://doi.org/10.1038/s41467-021-26321-9

Martinez, J. A., Kobayashi, M., Krishnan, A., Webber, C., Christie, K., Guo, G. F., Singh, V., & Zochodne, D. W. (2015). Intrinsic facilitation of adult peripheral nerve regeneration by the Sonic hedgehog morphogen. *Experimental Neurology*, *271*, 493–505. https://doi.org/10.1016/j.expneurol.2015.07.018

Mastrangelo, E., & Milani, M. (2018). Role and inhibition of GLI1 protein in cancer. *Lung Cancer (Auckland, N.Z.)*, *9*, 35–43. https://doi.org/10.2147/LCTT.S124483

Moradi, M., Hood, B., Moradi, M., & Atala, A. (2015). The potential role of regenerative medicine in the man-agement of traumatic patients. *Journal of Injury & Violence Research*, *7*(1), 27–35. https://doi.org/10.5249/jivr.v7i1.704

Nagumantri, S. P., Banu, S., & Idris, M. M. (2021). Transcriptomic and proteomic analysis of Hemidactylus frenatus during initial stages of tail regeneration. *Scientific Reports*, *11*(1), 3675. https://doi.org/10.1038/s41598-021-83283-0

Ninov, N., & Yun, M. H. (2015). Current advances in tissue repair and regeneration: the future is bright. *Regeneration*, *2*(2), 84–91. https://doi.org/10.1002/reg2.30

Novianti, T., Juniantito, V., Jusuf, A. A., Arida, E. A., Jusman, S. W. A., & Sadikin, M. (2019). Expression and role of HIF-1α and HIF-2α in tissue regeneration: a study of hypoxia in house gecko tail regeneration. *Organogenesis*, *15*(3), 69–84. https://doi.org/10.1080/15476278.2019.1644889

Piccioni, A., Gaetani, E., Neri, V., Gatto, I., Palladino, M., Silver, M., Smith, R. C., Giarretta, I., Pola, E., Hlatky, L., & Pola, R. (2014). Sonic hedgehog therapy in a mouse model of age-associated impairment of skeletal muscle regeneration. *The Journals of Gerontology. Series A, Biological Sciences and Medical Sciences*, *69*(3), 245–252. https://doi.org/10.1093/gerona/glt076

Sigafoos, A. N., Paradise, B. D., & Fernandez-Zapico, M. E. (2021). Hedgehog/GLI Signaling Pathway: Transduction, Regulation, and Implications for Disease. *Cancers*, *13*(14). https://doi.org/10.3390/cancers13143410

Straface, G., Aprahamian, T., Flex, A., Gaetani, E., Biscetti, F., Smith, R. C., Pecorini, G., Pola, E., Angelini, F., Stigliano, E., Castellot Jr., J. J., Losordo, D. W., & Pola, R. (2009). Sonic hedgehog regulates angiogenesis and myogenesis during post-natal skeletal muscle regeneration. *Journal of Cellular and Molecular Medicine*, *13*(8b), 2424–2435. https://doi.org/10.1111/j.1582-4934.2008.00440.x

Vonk, A. C., Zhao, X., Pan, Z., Hudnall, M. L., Oakes, C. G., Lopez, G. A., Hasel-Kolossa, S. C., Kuncz, A. W. C., Sengelmann, S. B., Gamble, D. J., & Lozito, T. P. (2023). Single-cell analysis of lizard blastema fibroblasts reveals phagocyte-dependent activation of Hedgehog-responsive chondrogenesis. *Nature Communications*, *14*(1), 4489. https://doi.org/10.1038/s41467-023-40206-z